Microchimica Acta (2018) 185: 420
https://doi.org/10.1007/s00604-018-2952-x

ORIGINAL PAPER

# Functional ZnS:Mn(II) quantum dot modified with L-cysteine and 6-mercaptonicotinic acid as a fluorometric probe for copper(II)

Jiangru Wang[1,2] · Jialuo Yu[2] · Xiaoyan Wang[2,3] · Liyan Wang[2] · Bowei Li[2] · Dazhong Shen[1] · Qi Kang[1] · Lingxin Chen[2,4]

Received: 25 May 2018 / Accepted: 3 August 2018 / Published online: 18 August 2018


## Abstract

Manganese-doped ZnS quantum dots (ZnS:Mn(II) QDs) were synthesized and modified with L-cysteine (L-Cys) and 6-mercaptonicotinic acid (MNA). This prevents the aggregation of the QDs and makes them available for the interaction with Cu(II) ions via Cu(II)-S interaction. As a result, the fluorescence of the QDs is quenched by Cu(II) due to an electron transfer mechanism. The QDs display two emission peaks under 325 nm excitation, one (being red) peaking at 593 nm, the other (blue) at 412 nm. The red fluorescence is strongly quenched, while the blue fluorescence is not affected. An easily distinguishable color change from orange red to purple can be observed in fluorescence as the concentration of Cu(II) is increased. The probe is selective over commonly encountered other ions. The ratio of fluorescence intensities at 593 and 412 nm increases linearly in the 5 to 500 nM Cu(II) concentration range, and the detection limit is 1.2 nM.

**Keywords** Copper ions · Nanoparticles · Fluorescent detection · Ratiometric fluorescence · Quenching · Dual emission · Water-soluble · Water samples · Manganese-doped ZnS · Electron transfer · Functionalization

## Introduction

Copper is an indispensable trace element of human health. It plays an important role in many biological processes [1]. However, excessive Cu(II) is also regarded as potentially toxic and endangers health [1–3]. The U.S. Environmental Protection Agency (EPA) has stipulated that the concentration of Cu(II) ions should be below 1.3 ppm (about 20 μM) in drinking water [4]. The recognition and detection of Cu(II) in environmental water samples is of great importance for water pollution monitoring. A number of analytical methods have been utilized for Cu(II) determination, including atomic absorption spectrometry [5], inductively coupled plasma-mass spectrometry (ICP-MS) [6], electrochemical method [7], colorimetry [8], and fluorometry [9]. Amongst them, fluorometry has gained popularity because of its simplicity, high efficiency and capability of real-time monitoring as well as high sensitivity and selectivity.

Various fluorescence substances are available for the fluorescence detection, such as organic dyes [10–12], carbon dots [13, 14], quantum dots (QDs) [15–19], silicon nanoparticles [20, 21] and metal nanoclusters [22]. Single wavelength fluorescence intensity is usually used as detection value, but it can be influenced by stability of light source, solution composition and environmental factors. Fortunately, ratiometric fluorometry can avoid these problems effectively [23], in which the ratio values of

Jiangru Wang and Jialuo Yu contributed equally to this work.

**Electronic supplementary material** The online version of this article (https://doi.org/10.1007/s00604-018-2952-x) contains supplementary material, which is available to authorized users.

✉ Qi Kang
kangqi@sdnu.edu.cn

✉ Lingxin Chen
lxchen@yic.ac.cn

1 College of Chemistry, Chemical Engineering and Materials Science, Shandong Normal University, Jinan 250014, China

2 CAS Key Laboratory of Coastal Environmental Processes and Ecological Remediation; Research Center for Coastal Environmental Engineering and Technology, Yantai Institute of Coastal Zone Research, Chinese Academy of Sciences, Yantai 264003, China

3 School of Pharmacy, Binzhou Medical University, Yantai 264003, China

4 College of Chemistry and Chemical Engineering, Qufu Normal University, Qufu 273165, China

fluorescence intensities from different wavelengths change along with analytes' concentrations changing [24]. Through establishing the internal standard, it greatly reduces the interference of other factors and effectively improves the accuracy of detection. The precondition for constructing a fluorometric ratiometric system is the dual-emission structure. Three common methods are usually adopted to synthesize ratiometric fluorescent materials as below. One is to synthesize energy transfer-based systems in which the energy transfer occurs from one (the donor) to the other (the acceptor) on the basis of FRET [10, 12]. When the emission spectrum of fluorescent donor overlaps the absorption spectrum of fluorescent acceptor for FRET, detection is highly efficient. The second ratiometric system is constructed by two independent luminophores with the same excitation wavelength [13]. Detection is based on two signals: one is analyte dependent and the other used as the stable internal reference. The above two methods use QDs or organic dyes as fluorescence signals and there must be two fluorescent materials for dual emissions. Interestingly, the third method is more convenient to form intrinsic dual emission from single QDs [16]. Usually, in this third method transition metals are doped into QDs (like ZnS, ZnSe, etc.) to obtain the intrinsic dual-emission QDs and they offer new opportunities for promising ratiometric sensing [25].

We describe here functional manganese-doped ZnS QD (ZnS:Mn(II) QD) nanoparticles for visual ratiometric fluorescent detection of Cu(II) ions in aqueous solutions. The ZnS:Mn(II) QDs as fluorescent signals are environmentally friendly and simple in preparation, moreover, they have excellent thermal stability and fluorescence properties compared to other heavy metals ion-based QDs. The surfaces of ZnS:Mn(II) QDs were modified by L-cysteine (L-Cys) and 6-mercaptonicotinic acid (MNA) to realize the functionalization of nanoparticles, which can detect Cu(II) ions based on an electron transfer-induced fluorescence quenching mechanism. The functional ZnS:Mn(II) QD fluorometric probe was well characterized and related experimental conditions were systematically investigated. Under the optimal conditions, the probe for Cu(II) assay was validated, and then was successfully applied to environmental water samples analysis.

## Experimental section

### Reagents and materials

Copper sulfate pentahydrate ($CuSO_4 \cdot 5H_2O$), absolute ethanol, acetonitrile, zinc acetate ($Zn(CH_3COO)_2 \cdot 2H_2O$), sodium sulfide ($Na_2S \cdot 9H_2O$), potassium chloride (KCl), calcium sulfate dihydrate, mercury chloride ($HgCl_2$), lead nitrate ($Pb(NO_3)_2$), nickel chloride ($NiCl_2$), cobalt chloride ($CoCl_2$), magnesium chloride ($MgCl_2$), cadmium nitrate tetrahydrate, sodium chloride (NaCl) and phosphate buffered saline (PBS, 0.01 M, consisting of 8 mM of $Na_2HPO_4$, 136 mM of NaCl, 2 mM of $KH_2PO_4$ and 2.6 mM of KCl) were obtained from Sinopharm Chemical Reagent Co., Ltd. (http://en.reagent.com.cn/). Manganese chloride ($MnCl_2$) and ferric chloride hexahydrate ($FeCl_3 \cdot 6H_2O$) were supplied by Aladdin (http://www.molbase.com/en/supplier-8759.html). L-cysteine (L-Cys) and 6-mercaptonicotinic acid (MNA) were purchased from Sigma-Aldrich (https://www.sigmaaldrich.com/china-mainland/promotions/new.html). All reagents and materials were of at least analytical pure grade and used directly without further purification. All aqueous solutions throughout the experiment were prepared with ultrapure water (18.2 MΩ cm), which was produced by a Milli-Q Ultrapure water system (Millipore, Bedford, MA, USA; https://www.yelp.com/biz/millipore-corporation-bedford).

### Instrumentation

The fluorescence spectrometer (FluoroMax-4, Horiba Scientific Corporation; https://www. ampdirectory.com/company/351024/horiba-scientific) was used for fluorescence detection. Ultraviolet-visible spectrophotometer (NanoDrop 2000/2000C, Thermo Fisher Scientific, USA; https://www.fishersci.com/us/en/home.html) was used to measure the UV-Vis absorption spectra. Morphology was observed by transmission electron microscopy (TEM, JEM-1230, JEOL, Japan; https://www.enfsolar.com/directory/equipment/21516/jeol) with operating voltage at 100 kV. The energy dispersive spectrum (EDS) was measured by a scanning electron microscope (SEM, Hitachi S-4800 FE-SEM, operating at 5 kV; https://www.enfsolar.com/directory/equipment/21516/jeol) equipped with an EDAX-PHOE-NIX energy spectrum probe. Elemental analysis was performed using a Vario Micro-cube elementar analyzer (Elementar Company, Germany; https://www.elementar.de/en/products.html). Fourier transform infrared (FT-IR) spectrometer (Thermo Nicolet Corporation, USA; https://www.machinio.com/manufacturer/nicolet#results) was employed to record the infrared spectra of samples, using a pressed KBr tablet method. X-ray photoelectron spectroscopy (XPS) measurements were taken on an ESCALAB $Xi^+$ spectrometer (Thermo Scientific, USA; https://www.thermofisher.com/cn/zh/home.html). ICP-MS analyses were performed on a Perkin Elmer ElanDRC II (USA; http://www.speciation.net/Database/Instruments/PerkinElmer-SCIEX/ELAN-DRC-II-; i183).

## Synthesis and modification of ZnS:Mn(II) QDs

Water-soluble ZnS:Mn(II) QDs were synthesized according to that reported process [26]. Specific synthesis process details can be found in Experimental S1 **Synthesis of ZnS:Mn(II) QDs**. The surface modification process of the ZnS:Mn(II) QDs is shown in Fig. 1. The specific steps were as follows: Take 5 mL of the above-mentioned synthetic ZnS:Mn(II) QDs solution diluted in 30 mL of ultrapure water. Then 14 mg of MNA and 13 mg of L-Cys were added while stirring for 12 h in the dark. The product was separated from the mixture with centrifugation and washed three times with ultrapure water and then stored in 30 mL of ultrapure water to obtain the complex QDs nanoparticles modified by MNA and L-Cys, i.e., MNA-L-Cys-ZnS:Mn(II) QDs.

## Fluorometric detection

The ratio of fluorescence emission peaks at 593 and 412 nm of the MNA-L-Cys-ZnS:Mn(II) QDs was used to detect the concentrations of Cu(II) ions in the aqueous solution. The slit widths of excitation and emission were both set at 9 nm, respectively. The excitation wavelength was set at 325 nm, and the emission spectrum was measured from 350 to 620 nm. In experiment the same amount of MNA-L-Cys-ZnS:Mn(II) QDs were taken at the concentration of 0.14 mg/mL. The changes of fluorescence intensity caused by different concentrations of Cu(II) ions were recorded.

## Actual environmental water samples analysis

Water samples were utilized to examine the practical applicability of the MNA-L-Cys-ZnS:Mn(II) QDs for the Cu(II) ions detection. Four different environmental water samples from the coastal zone region of the Urban District in Yantai City were collected into a Teflon bottle, including surface seawater samples from the Fisherman's Wharf of the Yellow Sea, lake water samples from an artificial lake, swimming pool water from a indoor swimming pool, and river water from a river nearby living quarters and industrial parks. The water samples were all filtrated with 0.45 μm microfiltration membrane to remove the suspended particles before use.

During the analytical procedure, all water samples were diluted 100-fold and then the diluted sample solutions were added different concentrations of Cu(II) ions for fluorescence detection. Specific steps were as follows. In a 1.5 mL of centrifuge tube, adding 880 μL of PBS buffer solution with pH of 6 (0.01 M) and 100 μL of MNA-L-Cys-ZnS:Mn(II) (measured at a concentration of 0.14 mg/mL). Then 10 μL of different concentrations of Cu(II) and different environmental water samples were added, respectively. The spiked concentrations of Cu(II) ions were 50, 100 and 250 nmol/L, respectively. The total volume of solution was kept at 1 mL. The mixture was shaken evenly and incubated for 7 min before fluorescence measurement. The specific measuring steps were at below. The testing solution consisted of 890 μL of PBS buffer solution with pH of 6 (0.01 M) and 100 μL of MNA-L-Cys-ZnS:Mn(II) (0.14 mg/mL), followed by adding 10 μL

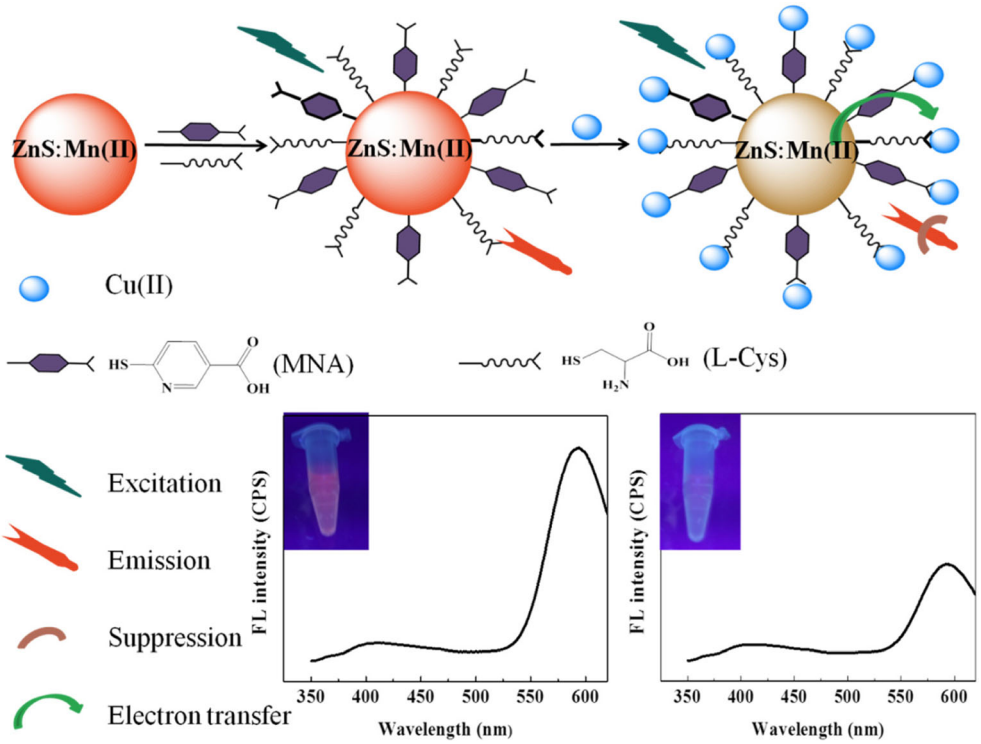


**Fig. 1** Preparation process of MNA-L-Cys-ZnS:Mn(II) nanoparticles and the possible mechanism for fluorescence detection of Cu(II)

of different concentrations of Cu(II) ions. The linear equation between Cu(II) ions concentration and fluorescence ratio ($I_{593}/I_{412}$) was obtained, namely, $(I_{593}/I_{412})_0/(I_{593}/I_{412}) = 1.0388 + 0.0019\times[Cu^{2+}]$. Then the concentrations of Cu(II) ions in the environmental water samples would be obtained according to the linear equation. The above steps were repeated three times, and the final average test results were compared with ICP-MS results.

## Results and discussion

### Preparation and possible detection mechanism of functional ZnS:Mn(II) QDs

ZnS:Mn(II) QDs were used as luminescent materials to build fluorescent nanoparticles with dual emission peaks for detection of Cu(II) ions. The preparation procedure and possible detection mechanism was shown in Fig. 1. The ZnS QDs have lower environmental toxicity than other semiconductor materials QDs such as CdTe, CdSe and CdS QDs. The stable MNA-L-Cys-ZnS:Mn(II) nanoparticles were prepared by synthesizing water-soluble ZnS:Mn(II) QDs in the aqueous phase and modifying MNA and L-Cys on the surface. The condition of synthesis was really mild and simple. In the synthesis process, $Zn(CH_3COO)_2{\cdot}2H_2O$ and $Na_2S{\cdot}9H_2O$ were equimolar, and the molar ratio of manganese ions dopant was 6%.

L-Cys was non-toxic and widely used in modification of water-soluble fluorescent nanoparticles [27]. The mercapto group of L-Cys bonded with ZnS:Mn(II) QDs by covalent bonds. The carboxyl group at the other end makes the water solubility of nanoparticles and it coordinates the metal ions, applied to the detection of metal ions [28]. Different from other mercapto linear small molecule such as mercapto carboxylic acid, mercaptoalcohol and mercapto amine, MNA contains a six-membered heterocyclic ring and a carboxyl group. With stronger acting force and stability, MNA can detect metal ions more sensitively. In the MNA molecule, both the sulfhydryl group and the nitrogen atom on the pyridine ring can interact with the ZnS QDs. At the same time, the nitrogen atom on the pyridine ring and the carboxyl acid group can also participate in the chelation with Cu(II) ions. However, when there were only the MNA molecules, they would recline on the surface of ZnS QDs due to the interaction between sulphur atom, nitrogen atom and ZnS. This greatly reduced the surface coverage utilization of ZnS QDs and was not conducive to ion detection. In contrast, interestingly, when both MNA and L-Cys were simultaneously modified, as illustrated in Fig. 1, the linear L-Cys may be competitively linked to the surface of QDs and thereby caused the MNA molecule in a vertical position in favor of MNA releasing nitrogen atoms to chelate with more Cu(II) ions. As well, L-Cys chelated with Cu(II) (Fig. 1). The larger amounts of MNA and L-Cys molecules were modified on the surface of ZnS:Mn(II) QDs to greatly increase the surface coverage and the amounts of chelated Cu(II). Obviously, the functionalization by L-Cys and MNA prevented the aggregation of the ZnS:Mn(II) QDs and made them available for the interaction with Cu(II) ions via Cu(II)-S interaction. Therefore, the MNA-L-Cys-ZnS:Mn(II) QDs can be expected to become an environmentally friendly and highly efficient material for copper(II) detection.

The MNA-L-Cys-ZnS:Mn(II) QDs have two fluorescence emission peaks under 325 nm excitation, as shown in Fig. S1a. The weaker blue emission peak at about 412 nm was the defect emission peak of the zinc sulfide matrix, while the strong red peak at about 593 nm corresponds to the characteristic emission of the energy level transition between $^4T_1$ to $^6A_1$ for manganese-doped ZnS [29, 30]. Mn(II) had an electron layer structure of 1 $s^2 2s^2 2p^6 3s^2 3p^6 3d^5$ and a ground state spectrum of $^6S_{5/2}$. It was known from the electron transition rule that the transition on the $d^5$ electron layer was banned. However, because of Mn(II) doped into the lattice of zinc sulfide crystals, the Zn(II) ions sites were partially substituted. The electronic structure changed due to the effect of the surrounding crystal field thus lifting part of the transition ban, at the same time achieving energy level transition of Mn(II) internal electron between $^4T_1$ to $^6A_1$ and fluorescence emission of red light. It showed that Mn(II) ions had replaced Zn(II) ions into the lattice of ZnS crystal to form ZnS:Mn(II) QDs. Compared with the defect-related emission of ZnS, the fluorescence emission band of QDs doped ions was more stable and more controllable because the defect peaks of semiconductor nanoparticles were easily affected by the synthesis process or environmental factors.

Fig. S1b shows the UV absorption spectra of MNA-L-Cys-ZnS:Mn(II) in the absence and presence of different concentrations of Cu(II) ions. As observed, absorption spectra were completely overlapped. As well, the fluorescence quenching of MNA-L-Cys-ZnS:Mn(II) occurred with the addition of different concentrations of Cu(II) ions, without emission-peak shift (Fig. S1a). These absorption and emission spectra can indicate no new products such as CuS were formed, different from [19]. In [19], the Cu(II) ions can displace the Zn(II) ions to form CuS and change the surface state of ZnS:Mn(II). The CuS cannot be fluorescent so the displayed photoluminescence intensity at 585 nm reduced with the addition of Cu(II) ions. In our work, the fluorescence quenching mechanism was assumed to be an electron transfer process between MNA-L-Cys-ZnS:Mn(II) and Cu(II) ions but not through the formation of CuS particles. As illustrated in Fig. 1, in the presence of Cu(II) ions, the carboxyl acid groups of the L-Cys molecule, the nitrogen atom on the pyridine ring and carboxyl acid groups in the MNA molecule all can participate in the coordinate bond of Cu(II) ions, leading to electron-transfer induced fluorescence quenching [31, 32].

So, a significantly quenching of the fluorescence intensity at approximately 593 nm would be observed. Under a UV lamp, the MNA-L-Cys-ZnS:Mn(II) QDs showed remarkable color change from orange red to purple (Fig. 1). Notably, since MNA-L-Cys-ZnS:Mn(II) QDs were well water-soluble and little amount was used, so that they cannot be centrifuged and reused. Consequently, the MNA-L-Cys-ZnS:Mn(II) QDs material was irreversible and can be regarded as a single shot probe. Therefore, the MNA-L-Cys-ZnS:Mn(II) fluorometric probe can be applied to the selective recognition and visual ratiometric fluorescent detection of Cu(II) ions.

## Characterization of the functional ZnS:Mn(II) QDs

The MNA-L-Cys-ZnS:Mn(II) QDs were characterized by TEM, EDS, elemental analysis, FT-IR and XPS. As shown in Fig. S2A, the ZnS:Mn(II) QDs were spherical in shape and had good dispersibility, and the particle size was about 3−5 nm. As seen from Fig. S2B, the MNA-L-Cys-ZnS:Mn(II) nanoparticles were similar to ZnS:$Mn^{2+}$ QDs in morphology and particle size distribution were more uniform. There wasn't obvious phenomenon of agglomeration.

EDS analysis was performed to further confirm the surface characteristic of the MNA-L-Cys-ZnS:Mn(II) QDs, as recorded in Fig. S3 and Table S1. The presence of S, Zn and Mn suggested the ZnS:Mn(II) QDs were used as support materials for surface modification to produce MNA-L-Cys-ZnS:Mn(II). The obviously increased percentage of carbon (24.80%) and decreased percentage of manganese (0.68%) for MNA-L-Cys-ZnS:Mn(II), as listed in Table S1, might well result from the modification by both MNA and L-Cys, and suggested the occurrence of surface functionalization. Furthermore, elemental analysis was carried out to examine the contents of N, C, H and S. As listed in Table S2, compared with the atomic composition of nitrogen (0.019%), carbon (0.603%), hydrogen (0.974%) and sulfur (26.886%) for ZnS:Mn(II) QDs, the obviously increased percentages of nitrogen (1.014%) and carbon (3.552%) for MNA-L-Cys-ZnS:Mn(II) revealed that MNA and L-Cys were successfully introduced onto the surface of ZnS:Mn(II) QDs. These experimental data provided direct evidences on the chemical modification of the probe.

In order to test whether the modification was successful, the FT-IR spectra of ZnS:Mn(II) QDs (Fig. 2a) and MNA-L-Cys-ZnS:Mn(II) nanoparticles (Fig. 2b) were recorded. By comparing the two kinds of spectra, the peaks at 3239 $cm^{-1}$ and 2919 $cm^{-1}$ (Fig. 2b) corresponding to the vibration absorption of the N-H bond proved that the amino groups were successfully introduced into the surface of the ZnS QDs. And the peaks at 1616 $cm^{-1}$ and 790 $cm^{-1}$ showed obvious characteristic peaks of the aromatic hydrocarbon (Fig. 2b). At the same time, as seen from Fig. 2b,c and d, the FT-IR absorption band around 1400 $cm^{-1}$ (−COO) can also successfully illustrate that ZnS:Mn(II) QDs was modified by MNA and L-Cys. On the other hand, the characteristic absorption peaks of the mercapto group (-SH) at 2550−2700 $cm^{-1}$ of MNA and L-Cys (Fig. 2c and d) disappeared in MNA-L-Cys-ZnS:Mn(II) (Fig. 2b), because the mercapto group and the surface of ZnS were easy to be covalently bonded. The above phenomena confirmed that MNA and L-Cys were successfully modified on the surface of ZnS:Mn(II) QDs.

The surface composition and elemental analysis for the MNA-L-Cys-ZnS:Mn(II) were also examined by XPS. The survey spectra (Fig. 3a) clearly showed six peaks at 162.3, 286, 401.8, 534.1, 655.8 and 1026.3 eV, which can be attributed to S 2p, C 1 s, N 1 s, O 1 s, Mn 2p, and Zn 2p, respectively. A high-resolution XPS spectrum of N 1 s (Fig. 3b) confirmed the presence of C−$NH_2$, implying that the amino groups were partly doped into the ZnS:Mn(II) QDs. The two almost symmetrical peaks at 286 and 288.5 eV in C 1 s spectrum (Fig. 3c) may be assigned to C−OH and O−C=O groups, respectively. The surface components of the MNA-L-Cys-ZnS:Mn(II) determined by the XPS were in good agreement with FT-IR results.

## Fluorescence properties of the functional ZnS:Mn(II) QDs

The fluorescence spectra of ZnS:Mn(II) QDs and MNA-L-Cys-ZnS:Mn(II) under 325 nm excitation were shown in Fig. 4. Compared to ZnS:Mn(II) QDs (Fig. 4a), the fluorescence intensity of MNA-L-Cys-ZnS:Mn(II) probe at 593 nm slightly decreased but the peak position was basically invariable (Fig. 4b), possibly because the surface was modified with MNA and L-Cys. Due to the size effect of the QDs, the emission peak of the blue light part of the ZnS was partially blue shifted, but intensity was basically invariable. After modification, the MNA-L-Cys-ZnS:Mn(II) nanoparticles had two obvious fluorescence emission peaks at 593 and 412 nm (Fig. 4b) for ratiometric fluorescence analysis.

Herein, the choice of 325 nm as an excitation wavelength was based on the following reasons. If working in the UV ($\lambda_{exc}$ = 310 nm) makes the probe prone to interferences by biomatter (in blood/serum, cells, marine water, wastewaters etc.) which always display strong background UV absorption and fluorescence. In addition, the UV light used for excitation may be screened off by UV absorbing molecules. On the other hand, if an excitation wavelength of around 400 nm is used, the adverse inner filter effects in the UV easily interfere with the detection. Furthermore, by examining the fluorescence excitation spectra of MNA-L-Cys-ZnS:Mn(II) at emission wavelength of 593 and 412 nm (Fig. S4) as well as the probe's fluorescence emission spectra at the excitation wavelength of 360, 400 and 325 nm (Fig. S5), it can be concluded that 325 nm is the optimal selection as an excitation wavelength of the MNA-L-Cys-ZnS:Mn(II) nanoparticles.

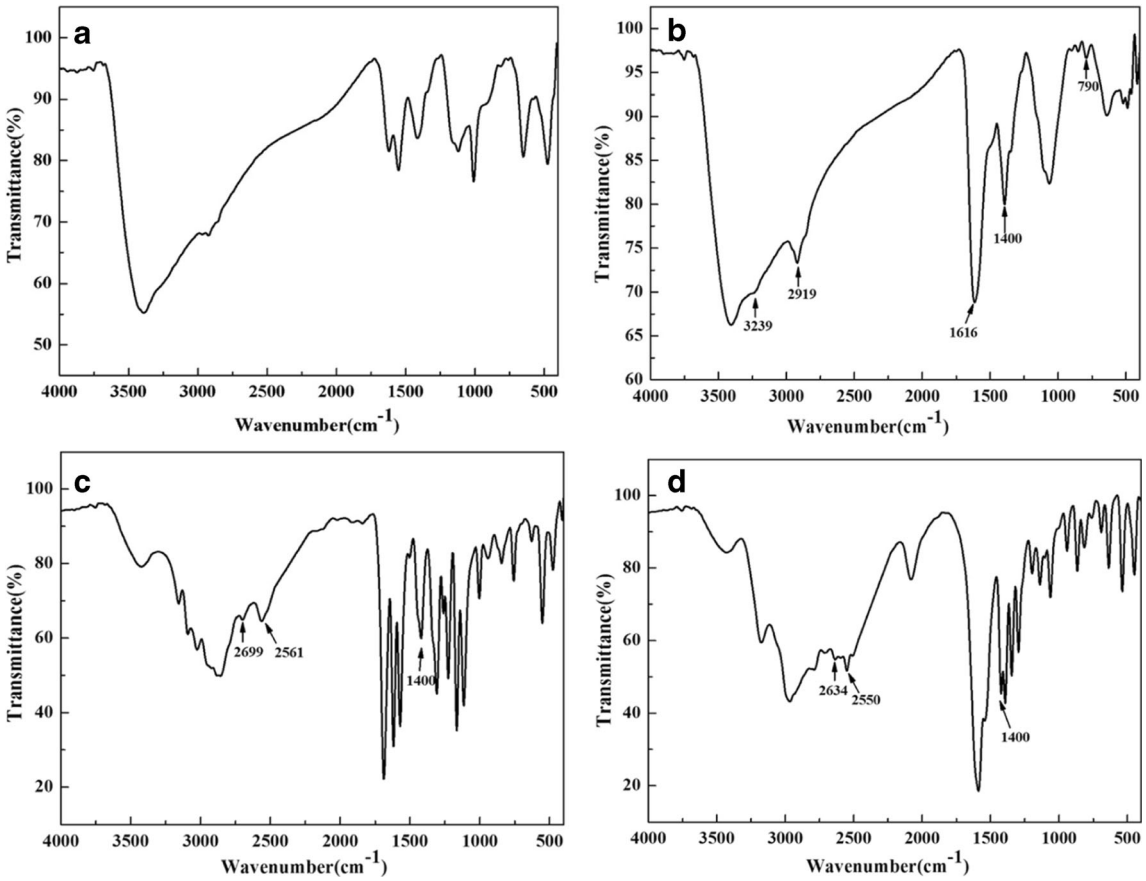


**Fig. 2** FT-IR spectra of (**a**) ZnS:Mn(II) QDs, (**b**) MNA-L-Cys-ZnS:Mn(II), (**c**) MNA and (**d**) L-Cys

In order to attain ideal fluorescence properties, the following parameters were optimized: (a) sample pH value; (b) reaction time; (c) concentration (or amount) of MNA-L-Cys-ZnS:Mn(II) QDs and (d) reaction temperature. The changing curve of fluorescence intensity ratio ($I_{593}/I_{412}$) combined with MNA-L-Cys-ZnS:Mn(II) and Cu(II) ions was measured in the range of pH 5.0–9.0. As shown in Fig. S6A, achieving the best effect of fluorescence quenching at pH = 6. In acidic medium, the fluorescence intensity significantly reduced due to the protonation of bonded mercapto group and carboxyl group on the surface of ZnS:Mn(II) QDs. With the increase of pH, deprotonation of L-Cys and MNA molecules was obvious. This deprotonation reinforces the covalent binding force between the ZnS:Mn(II) QDs with the MNA and L-Cys, and as a result the effect of fluorescence quenching was enhancing [27, 33]. However, while the pH was higher and the alkalinity was stronger, the effect of fluorescence quenching was reduced due to the generation of $Cu(OH)_2$ precipitation [34]. Therefore, in this work, we selected pH at 6 as the appropriate pH, and further experiments were operated in 0.01 M of PBS buffer solution at pH = 6.

The reaction time of combined MNA-L-Cys-ZnS:Mn(II) nanoparticles with Cu(II) ions was investigated. As seen from Fig. S6B, the fluorescence intensity of the emission peak at 593 nm decreased rapidly in 4 min, and then the curve tended to be stable. Such short reaction time enabled rapid and efficient detection of Cu(II) ions. In order to ensure the sufficient reactions, 7 min was selected in the subsequent experiments.

The amount of MNA-L-Cys-ZnS:Mn(II) was optimized by using 50, 100, 150, 200, 250 and 300 μL of the MNA-L-Cys-ZnS:Mn(II). As seen from Fig. S6C, at 100 μL, the highest ratio value was attained in favor of Cu(II) ion detection. At lower or higher amount, the ratio values remarkably decreased. So, 100 μL of MNA-L-Cys-ZnS:Mn(II) was used in this work; that is, the probe concentration was 0.14 mg/mL during the experiment. As well, the effect of temperature was examined. Three concentrations of Cu(II) ions (50, 100, 250 nM) were employed, and three different temperature value (25, 37 and 45 °C) were used for reaction. As observed from Fig. S6D, at 25 °C i.e. usually room temperature, the optimal detection value was demonstrated. As a result, the probe experiment was carried out at 25 °C, making the operation quite convenient and simple.

Consequently, the following experimental conditions were found to give best results: (a) best sample pH value: 6; (b) optimal reaction time: 7 min; (c) optimal amount (or concentration) of MPA-ZnS:Mn QDs(II): 100 μL (0.14 mg/mL) and (d) best reaction temperature: 25 °C.

Under the above optimal conditions, the long-term stability, anti-photobleaching and antioxidation of the MNA-L-Cys-

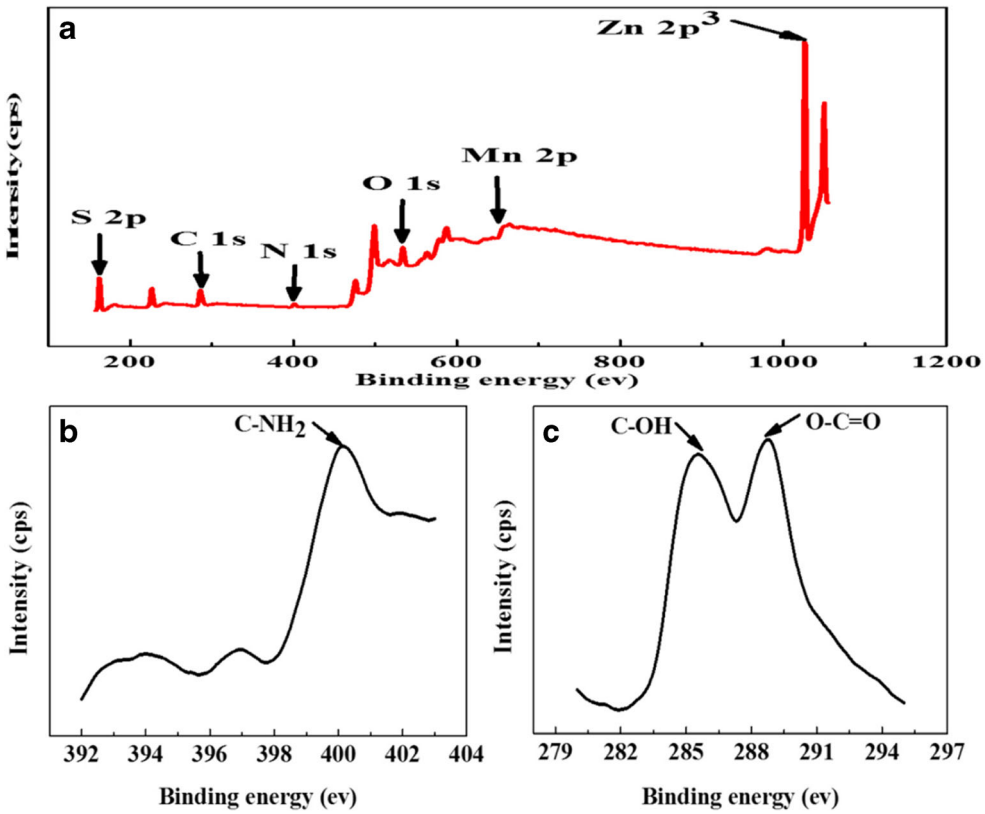


**Fig. 3** XPS spectra of MNA-L-Cys-ZnS:Mn(II): (**a**) survey, (**b**) N 1 s and (**c**) C 1 s

ZnS:Mn(II) probe were investigated. Fig. S7A shows the fluorescence ratio change by repeatedly detecting the fluorescence intensity when the place time was 1, 2, 3, 4, 5, 6, 7 and even 90 days. The emission was quite stable within 7 days. Furthermore, after the probe was stored at 4 °C in a refrigerator for 90 days, only slightly reduction was found in the detection results. The maintained fluorescence intensity within 7 days and 3 months showed the probe had excellent long-term stability, possibly owing to the surface medication by MNA and L-Cys. In addition, the results of Fig. S7B and 7C demonstrated the probe possessed super anti-photobleaching and antioxidation properties.

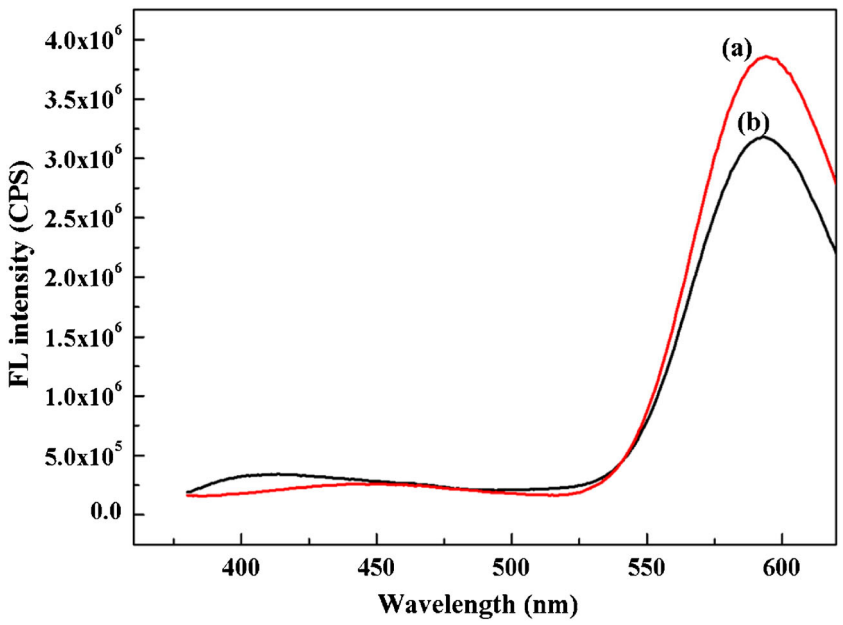


**Fig. 4** Fluorescence spectra of (**a**) ZnS:Mn(II) QDs and (**b**) MNA-L-Cys-ZnS:Mn(II)

## Sensitivity of the functional ZnS:Mn(II) QDs fluorometric probe for Cu(II)

The MNA-L-Cys-ZnS:Mn(II) ratiometric fluorescent nanoparticles had two fluorescence emission peaks at 412 and 593 nm, respectively. The fluorescence response of nanoparticles to Cu(II) ions was measured under the optimum experimental conditions. As shown in Fig. 5, with the increase of Cu(II) ions concentrations the fluorescence intensity of red emission peak at 593 nm decreased while the blue emission peak at 412 nm remained essentially constant, and the ratio of fluorescence intensity ($I_{593}/I_{412}$) was continuously reduced. At the same time, the ratio changes between intensities of the two emission peaks caused variation of the fluorescence colors from orange red to purple (as shown in Fig. 5 inset graph) while the concentration of Cu(II) ions increased and can be visually observed. It can be seen from the inset graph that the ratio of fluorescence intensity ($I_{593}/I_{412}$) had a good linear relationship with the concentration of Cu(II) ions. The linear equation between Cu(II) ions concentration and fluorescence ratio values ($I_{593}/I_{412}$) was $(I_{593}/I_{412})_0/(I_{593}/I_{412}) = 1.0388 + 0.0019\times[Cu^{2+}]$, and the correlation coefficient was 0.9955 when the concentrations of Cu(II) ions were in the 5 to 500 nM Cu(II) concentration range. According to the triple signal-to-noise ratio rule, the detection limit was 1.2 nM, which was much lower than the safe limit of 20 μM for Cu(II) ions in drinking water regulated by EPA [4].

## Selectivity of the fluorometric probe for Cu(II)

In order to detect the selectivity of MNA-L-Cys-ZnS:Mn(II) to Cu(II) ions, the fluorescence intensity ratio ($I_{593}/I_{412}$) for other ions was also studied under the same conditions. As shown in Fig. 6a, the fluorescence intensity of red emission peak at 593 nm was quenched about 80.33 and 61.27% after adding Cu(II) ions with concentration of 100 and 250 nM, respectively, and obvious color changes were observed by the naked eyes (inset graph). By contrast, the fluorescence intensity and color of the other metal ions such as $Pb^{2+}$, $Hg^{2+}$, $Mn^{2+}$, $Cd^{2+}$, $Cd^{2+}$, $Zn^{2+}$, $Na^{+}$, $Fe^{3+}$, $Co^{2+}$, $Ca^{2+}$, $K^{+}$ and $Ni^{2+}$ didn't change when their concentrations were 100 nM individual. Thus, the MNA-L-Cys-ZnS:Mn(II) ratiometric fluorescent probe had high selectivity for the detection of Cu(II) ions.

Then, the influences of other metal ions when co-existing with Cu(II) on the probe for Cu(II) were further studied. The other possible co-existing metal ions including $Mn^{2+}$, $Mg^{2+}$, $Cd^{2+}$, $Zn^{2+}$, $Na^{+}$, $Fe^{3+}$, $Co^{2+}$, $Ca^{2+}$, $K^{+}$ and $Ni^{2+}$ were respectively added at 10 μM individual, 100 times higher than Cu(II) ions. $Pb^{2+}$ and $Hg^{2+}$ were respectively added at 0.5 μM, 5 times of Cu(II) ions. As shown in Fig. 6b, the probe was hardly affected. Considering $Ca^{2+}$ and $Mg^{2+}$ can be present in 100–1000-fold excess, 500 or 1000-fold of $Ca^{2+}$ and $Mg^{2+}$, was added separately or simultaneously, and no obvious influence on Cu(II) detection was found (Fig. S8). Furthermore, all the mentioned other ions were simultaneously added, individual at 0.1 fold or the same concentration of Cu(II), a slight ratio increase or higher increase of the probe occurred (Fig. S8). Since the simultaneous presence of ten more ions produced quite high ion strength, certain influence on the probe is normal. Nevertheless, considering the practical conditions, such as not all the ions co-existed, their individual concentrations weren't so high, and the ratio increase wasn't high, the probe still demonstrated high selectivity for Cu(II) and may reliably work when analyzing complex samples.

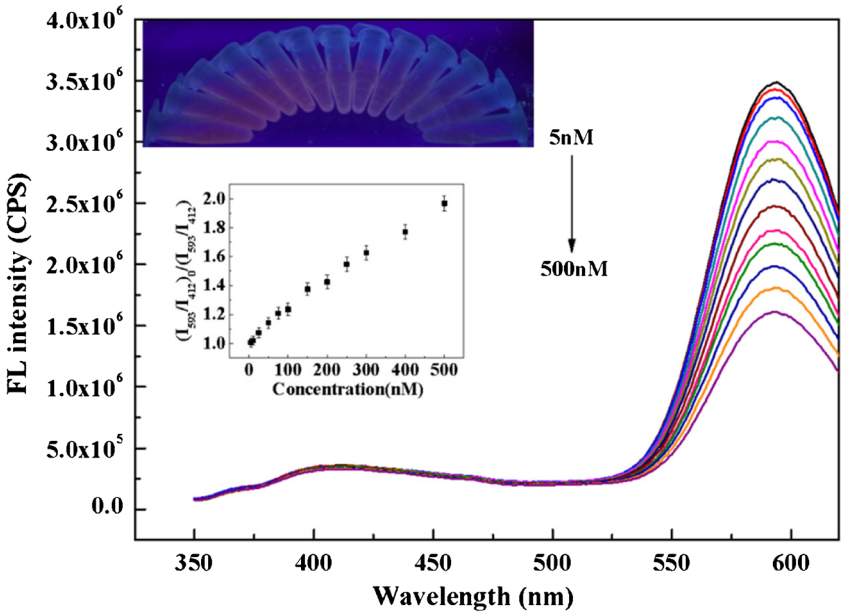


**Fig. 5** Fluorescence emission spectra of MNA-L-Cys-ZnS:Mn(II) with addition of Cu(II) ions at different concentrations. The inset graphs show the linear relationship between the fluorescence ratio value and the Cu(II) ions concentrations and the corresponding color changes

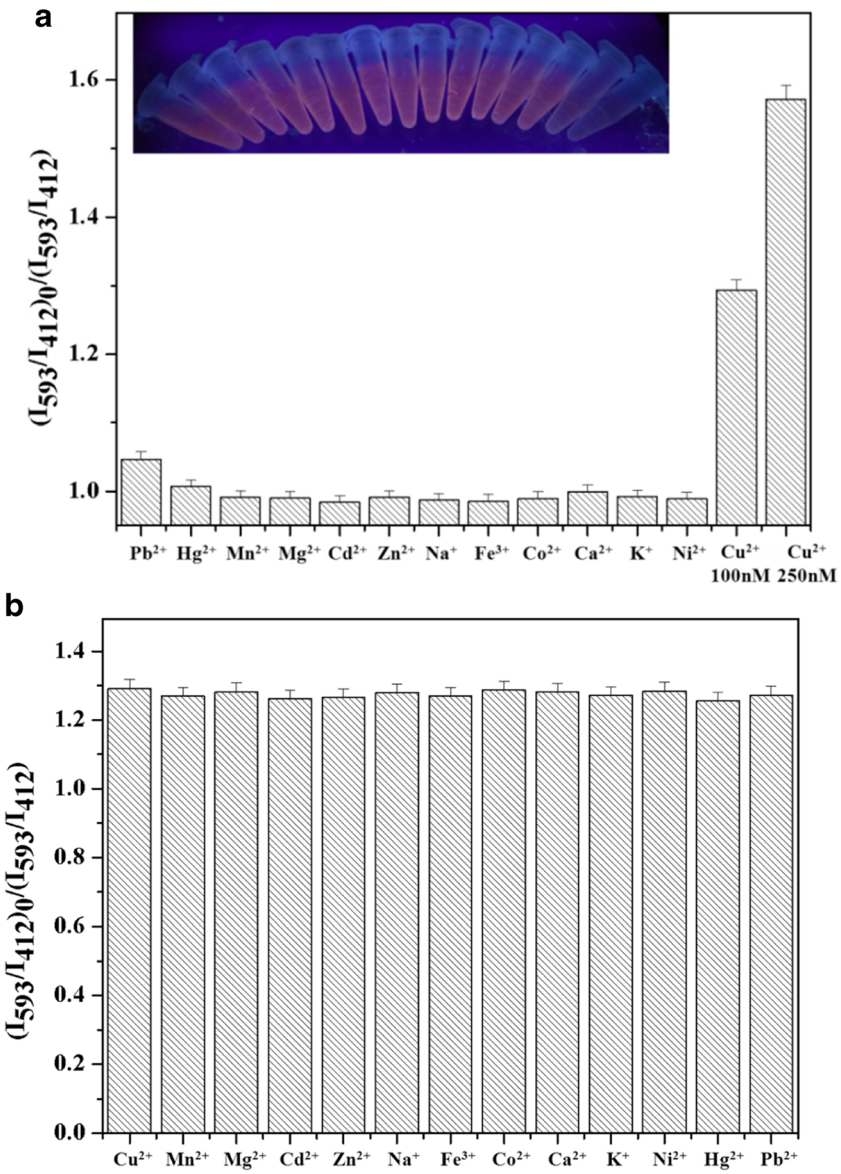


**Fig. 6** Selectivity of the functional ZnS:Mn(II) QDs nanoparticles for Cu(II). **a** Each metal ion was separately added into the reaction solution. The concentrations of Cu(II) ions were 100 nM and 250 nM, and the concentrations of the other metal ions were 100 nM each. The inset graph was the corresponding fluorescent color. **b** Cu(II) was added into the reaction system in the presence of other metal ions. The concentration of Cu(II) ions was 100 nM, the concentrations of the $Pb^{2+}$ and $Hg^{2+}$ ions were 0.5 μM, and the concentrations of the other metal ions were 10 μM each. The blank sample was the nanoparticles reaction system without adding any metal ions; data depict the average values from three independent experiments

## Application of the ratiometric fluorometric determination to environmental water samples

In order to further evaluate the practical application of the established analytical method, seawater, lake, swimming pool and river water samples were spiked with standard solutions containing different concentrations of Cu(II) and then detected. Before (spiking) detection, the 100-fold dilution procedure of the collected water samples was required to conduct. Otherwise great matrix interferences can make the probe invalid. The average recoveries were obtained with the relative standard deviations (RSDs) by measuring three triplicates for each concentration. Related experimental data are listed in Table 1. As seen, satisfactory recoveries were attained at 97.1–107.3% for the spiked seawater sample, 92.6–109.2% for the spiked lake water sample, and 90.2–106.3% for the spiked swimming pool water sample, respectively. The values of RSDs below 4.5% suggested the reliability and accuracy of the ratiometic fluorescence detection method. In addition, the results were comparable to that obtained by ICP-MS, namely, 89.5−108.3% for seawater sample, 89.1−106.3% for lake water sample, and 89.4−104.0% for swimming pool water sample, with RSDs less than 3.7%. It should be noted that no endogenous contents were found in all the above-three water samples. In contrast, as listed in Table 1, in river water sample, endogenous Cu(II) was detected at 8.986 μM by our present method, very consistent with that obtained by ICP-MS (9.320 μM). The *t*-test confirmed that there was no significant difference between the developed method and the ICP-MS determination at 95% confidence level. Although the value was less than the allowable 20 μM in drinking water by EPA, certain degree pollution still occurred, quite possibly

**Table 1** Results of spiked recoveries and RSDs (%; $n = 3$) for the detection of Cu(II) in seawater, lake water, swimming pool water and river water samples using the MNA-L-Cys-ZnS:Mn(II) probe and conventional ICP-MS.

| Samples | Spiked | MNA-L-Cys-ZnS:Mn(II) probe | | ICP-MS | |
|---|---|---|---|---|---|
| | (nM) | Recovery [a] (%) | RSD (%) | Recovery (%) | RSD (%) |
| Seawater | 50.0 | 101.0 | 3.7 | 89.5 | 3.7 |
| | 100.0 | 97.1 | 4.2 | 101.2 | 1.5 |
| | 250.0 | 107.3 | 4.5 | 108.3 | 3.1 |
| Lake water | 50.0 | 92.6 | 3.8 | 92.0 | 1.1 |
| | 100.0 | 109.2 | 4.1 | 106.3 | 3.7 |
| | 250.0 | 94.8 | 2.9 | 89.1 | 1.8 |
| Swimming pool water | 50.0 | 91.8 | 3.0 | 95.8 | 2.5 |
| | 100.0 | 106.3 | 3.8 | 89.4 | 2.5 |
| | 250.0 | 90.2 | 2.9 | 104.0 | 2.3 |
| River water[b] | 50.0 | 103.0 | 3.1 | 91.0 | 0.5 |
| | 150.0 | 112.8 | 4.2 | 90.3 | 0.9 |
| | 250.0 | 91.0 | 3.9 | 101.0 | 1.6 |

[a] Average value from three individual experiments

[b] Endogenous content of Cu(II) was found to be 9.320 μM by ICP-MS and 8.986 μM by the presented probe, respectively, which is the average value from three replicate tests

from the effluents of sanitary and industrial wastewater nearby. These good results in Table 1 confirmed that the MNA-L-Cys-ZnS:Mn(II) based method was practically applicable to the detection of Cu(II) ions in real water samples, demonstrating great potential for the routine analysis and monitoring of Cu(II).

## Comparison of method performance

The analytical performance of our MNA-L-Cys-ZnS:Mn(II) QDs method for detection of Cu(II) was compared with that of other reported nanomaterial-based fluorometric methods, as listed in Table 2 [4, 9, 13, 14, 18–22, 35, 36]. It can be seen that, all the nanomaterial systems are based on fluorescence quenching, which results from electron transfer. Most fluorometric methods present a wide quantitation span, good selectivity and real-sample feasibility. However, they also have some problems, such as a complicated synthesis [4, 35] or low sensitivity [9, 13, 14, 21, 36]. Although our synthesis procedure is slightly more complex than that reported [14, 19, 21, 22], excitingly, the detection limit is much better than that of reported methods [4, 9, 13, 14, 21, 22, 36]. In the research of [18], lower detection limit and wider linear rang is attained, however, the method is based on CdTe QDs (less eco-friendliness than ZnS QDs) and needs a passivation procedure. The ion imprinting based method offers higher selectivity, but the linear range is narrower (10–100 μM) and the lower-end quantitation concentration is quite high (10 μM) [20]. In addition, although it seems similar between [19] and our work, owing to the ZnS:Mn(II) QDs related nanoscale fluorescent probe for Cu(II) ions in water samples, in fact, there are obvious differences as follows. In [19], ZnS:Mn/$SiO_2$ QDs were synthesized by coating ZnS:Mn nanoparticles with silica shells through a microemulsion method, while in our work ZnS:Mn(II) QDs were firstly synthesized in aqueous phase using a chemical precipitation method, followed by modification with MNA and L-Cys in aqueous solutions, producing the functional MNA-L-Cys-ZnS:Mn(II) QDs. In [19], photoluminescence spectra/intensities at 585 nm emission peak of ZnS:Mn/$SiO_2$ QDs were used for single wavelength fluorescent detection, while in our work, the ratio of fluorescence intensities at 412 and 593 nm emission peaks in the MNA-L-Cys-ZnS:Mn(II) was used for ratiometric fluorescence detection. As well, our detection and quenching mechanism is different from [19]. Moreover, the lower-end quantitation concentration (5 nM) in the linear range of our work is much lower than that (81.6 nM) in [19], and the detection limit was down to 1.2 nM in our work, but without mentioning in [19]. Therefore, overall, our MNA-L-Cys-ZnS:Mn(II) probe method has many obvious advantages, such as high sensitivity and selectivity, wide linear range, simple operation, short analysis time, sensitive visualization and good practical applicability.

## Conclusions

A novel and effective MNA-L-Cys-ZnS:Mn(II) ratiometric fluorometric assay has been developed for the highly sensitive and selective detection of Cu(II) ions in aqueous solutions. The functionalization of ZnS:Mn(II) QDs with L-Cys and MNA endows the QDs with excellent fluorescence properties

**Table 2** Analytical performances comparison with other reported nanomaterial-based fluorometric methods for Cu(II) detection

| Nanomaterial systems | Linear range | Detection limit (nM) | Real samples | Ref. |
|---|---|---|---|---|
| Rhodamine B-based sensor | 1−10 nM | – | Human lung adenocarcinoma cells | [29] |
| ZPA[a] | 0−2000 nM | 14.9 nM | Tap water, lake water and waste water | [30] |
| DNA-Cu/Ag NC probe[b] | 5−200 nM | 2.7 nM | Soil and pond water | [4] |
| Fluorescent probe based on arhodamine spirolactame derivative | 50−900 nM | 7.0 nM | HeLa cells | [9] |
| BPEI-capped CQDs[c] | 10−1100 nM | 6 nM | River water | [13] |
| BPEI-CQDs[d] | 333 nM−66.6 μM | 115 nM | River water | [14] |
| Eu(III)@$SiO_2$@IPs[e] | 10–100 μM | – | River water | [20] |
| TAN-passivated CdTe QDs[f] | 23.3 nM–23.3 μM | 0.5 nM | Bovine serum albumin, fetal bovine serum | [18] |
| GSH-AuNCs[g] | 0–130 nM | 2.8 nM | Hep-2 cells, *E. coli* bacteria | [22] |
| SiNPs[h] | 0.05–15 μM | 29 nM | Tap water, mineral water, river water | [21] |
| ZnS:Mn(II)/$SiO_2$ QDs[i] | 81.6 nM−496 μM | – | Seawater | [19] |
| MNA-L-Cys-ZnS:Mn(II) QDs | 5−500 nM | 1.2 nM | Seawater, lake water, swimming water, river water | This work |

[a] Product was synthesized by $ZnTPPSNH_2$, 2-hydroxybenzaldehyde and acetic acid

[b] DNA-Cu/Ag nanocluster probe

[c] Branched poly (ethylenimine) (BPEI)-functionalized carbon quantum dots

[d] Branched polyethylenimine (BPEI)-carbon quantum dots

[e] Silica spheres doped with an Eu(III) complex and coated them with a nanoshell of a copper-imprinted polymer

[f] 1-(2-thiazolylazo)-2-naphthol (TAN) passivated CdTe nanocrystals

[g] Reduced glutathione stabilized and capped gold nanoclusters

[h] Silicon nanoparticles

[i] Silica-coated ZnS:Mn quantum dots

and makes the method simple, easy and rapid. Under the optimal conditions, a relative detection limit and a good linearity are attained, along with visualization detection. The method has demonstrated high selectivity towards Cu(II) ions with few responses to other metal ions. In addition, this method has been successfully applied to the detection of Cu(II) in real water samples and obtained satisfactory results, indicating its good practical application prospective. The ratiometric fluorescence method is beneficial to the application and development of doped QDs. On the other hand, it should be noted that this new MNA-L-Cys-ZnS:Mn(II) ratiometric fluorometric probe also has two major limitations. For real water sample analysis, the 100-fold dilution of the collected water samples is required; otherwise the great matrix interferences can make the probe invalid. The probe response is irreversible, which restricts the probe's reusability and online detection application. Nonetheless, this probe method still provides a good alternative for the detection of Cu(II) in water samples.

**Acknowledgments** This work was financially supported by the National Natural Science Foundation of China (21575080, 21275091, 41776110), Key Research and Development Plan of Shandong Province (GG201709290055), and the Science and Technology Development Plan of Yantai (2015ZH087, 2017ZH089).

**Compliance with ethical standards** The authors declare they have no competing interests.

## References

1. Kumawat LK, Mergu N, Singh AK, Gupta VK (2015) A novel optical sensor for copper ions based on phthalocyanine tetrasulfonic acid. Sensors Actuators B Chem 212:389–394
2. Jo J, Lee HY, Liu W, Olasz A, Chen CH, Lee D (2012) Reactivity-based detection of copper(II) ion in water: oxidative cyclization of azoaromatics as fluorescence turn-on signaling mechanism. J Am Chem Soc 134(38):16000–16007
3. Madsen E, Gitlin JD (2007) Copper and iron disorders of the brain. Annu Rev Neurosci 30:317–337
4. Su Y, Lan G, Chen W, Chang H (2010) Detection of copper ions through recovery of the fluorescence of DNA-templated copper/silver nanoclusters in the presence of mercaptopropionic acid. Anal Chem 82:8566–8572
5. Cassella RJ, Magalhães OIB, Couto MT, Lima ELS, Neves MAFS, Coutinho FMB (2005) Synthesis and application of a functionalized resin for flow injection/FAAS copper determination in waters. Talanta 67(1):121–128
6. Becker JS, Matusch A, Depboylu C, Dobrowolska J, Zoriy MV (2007) Quantitative imaging of selenium, copper, and zinc in thin sections of biological tissues (slugs-genus Arion) measured by laser ablationinductively coupled plasma mass spectrometry. Anal Chem 79:6074–6080
7. Smith SR, Zhou C, Baron JY, Choi Y, Lipkowski J (2016) Elucidating the interfacial interactions of copper and ammonia with the sulfur passive layer during thiosulfate mediated gold leaching. Electrochim Acta 210:925–934
8. Gao Q, Ji L, Wang QN, Yin K, Li JH, Chen LX (2017) Colorimetric sensor for highly sensitive and selective detection of copper ion. Anal Methods 9:5094–5100
9. Yu C, Zhang J, Li J, Liu P, Wei P, Chen L (2011) Fluorescent probe for copper(II) ion based on a rhodamine spirolactame derivative, and its application to fluorescent imaging in living cells. Microchim Acta 174(3−4):247−255
10. Goswami S, Sen D, Das NK (2010) A new highly selective, ratiometric and colorimetric fluorescence sensor for $Cu^{2+}$ with a remarkable red shift in absorption and emission spectra based on internal charge transfer. Org Lett 12(4):856–859
11. Yu C, Zhang J, Wang R, Chen L (2010) Highly sensitive and selective colorimetric and off-on fluorescent probe for $Cu^{2+}$ based on rhodamine derivative. Org Biomol Chem 8(23):5277–5279
12. Kamila S, Callan JF, Mulrooney RC, Middleton M (2007) A novel fluorescent chemosensor for cu(II) in aqueous solution based on a β-aminobisphosphonate receptor. Tetrahedron Lett 48(44):7756–7760
13. Dong Y, Wang R, Li G, Chen C, Chi Y, Chen G (2012) Polyamine-functionalized carbon quantum dots as fluorescent probes for selective and sensitive detection of copper ions. Anal Chem 84(14): 6220–6224
14. Liu Y, Zhao Y, Zhang Y (2014) One-step green synthesized fluorescent carbon nanodots from bamboo leaves for copper(II) ion detection. Sensors Actuators B Chem 196:647–652
15. Xie H, Liang J, Zhang Z, Liu Y, He Z, Pang D (2004) Luminescent CdSe-ZnS quantum dots as selective $Cu^{2+}$ probe. Spectrochim Acta A 60(11):2527–2530
16. Wang F, Gu Z, Lei W, Wang W, Xia X, Hao Q (2014) Graphene quantum dots as a fluorescent sensing platform for highly efficient detection of copper(II) ions. Sensors Actuators B Chem 190:516–522
17. Yu N, Peng H, Xiong H, Wu X, Wang X, Li Y, Chen L (2015) Graphene quantum dots combined with copper(II) ions as a fluorescent probe for turn-on detection of sulfide ions. Microchim Acta 182(13−14):2139–2146
18. Chao MR, Hu CW, Chen JL (2016) Fluorometric determination of copper(II) using CdTe quantum dots coated with 1(2-thiazolylazo)-2-naphthol and an ionic liquid. Microchim Acta 183(4):1323–1332
19. Qin JJ, Dong BH, Gao RJ, Su G, Han JW, Li X, Liu W, Wang W, Cao LX (2017) Water-soluble silica-coated ZnS:Mn nanoparticles as fluorescent sensors for the detection of ultratrace copper(II) ions in seawater. Anal Methods 9:322–328
20. Zheng XD, Pan JM, Gao L, Wei X, Dai JD, Shi WD, Yan YS (2015) Silica nanoparticles doped with a europium(III) complex and coated with an ion imprinted polymer for rapid determination of copper(II). Microchim Acta 182(3–4):753–761
21. Chen XG, Lu QJ, Liu D, Wu CY, Liu ML, Li HT, Zhang YY, Yao SZ (2018) Highly sensitive and selective determination of copper(II) based on a dual catalytic effect and by using silicon nanoparticles as a fluorescent probe. Microchim Acta 185(3):188 (7 pages)
22. Kong LC, Chu XF, Ling X, Ma GY, Yao YY, Meng YH, Liu WW (2016) Biocompatible glutathione-capped gold nanoclusters for dual fluorescent sensing and imaging of copper(II) and temperature in human cells and bacterial cells. Microchim Acta 183(7):2185–2195
23. Singh N, Kaur N, McCaughan B, Callan JF (2010) Ratiometric fluorescent detection of cu(II) in semi-aqueous solution using a two-fluorophore approach. Tetrahedron Lett 51(26):3385–3387
24. Cao B, Yuan C, Liu B, Jiang C, Guan G, Han M (2013) Ratiometric fluorescence detection of mercuric ion based on the nanohybrid of fluorescence carbon dots and quantum dots. Anal Chim Acta 786: 146–152
25. Wu P, Hou X, Xu J, Chen H (2016) Ratiometric fluorescence, electrochemilumine-scence, and photoelectrochemical chemo/biosensing based on semiconductor quantum dots. Nanoscale 8: 8427–8442

26. Zhang K, Yu T, Liu F, Sun M, Yu H, Liu B, Zhang Z, Jiang H, Wang S (2014) Selective fluorescence turn-on and ratiometric detection of organophosphate using dual-emitting Mn-doped ZnS nanocrystal probe. Anal Chem 86(23):11727–11733
27. Kho R, Torres-Martínez CL, Mehra RK (2000) A simple colloidal synthesis for gram-quantity production of water-soluble ZnS nanocrystal powders. Colloid Interf Sci 227(2):561–566
28. Koneswaran M, Narayanaswamy R (2009) L-cysteine-capped ZnS quantum dots based fluorescence sensor for $Cu^{2+}$ ion. Sensors Actuators B Chem 139(1):104–109
29. Lu L, Yang G, Xia Y (2014) From pair to single: sole fluorophore for ratiometric sensing by dual-emitting quantum dots. Anal Chem 86(13):6188–6191
30. Zhang K, Yang L, Zhu H, Ma F, Zhang Z, Wang S (2014) Selective visual detection of trace trinitrotoluene residues based on dual-color fluorescence of graphene oxide–nanocrystals hybrid probe. Analyst 139(10):2379–2385
31. Duan J, Jiang X, Ni S, Yang M, Zhan J (2011) Facile synthesis of n-acetyl-l-cysteine capped zns quantum dots as an eco-friendly fluorescence sensor for $Hg^{2+}$. Talanta 85(4):1738–1743
32. Lou Y, Zhao Y, Chen J, Zhu JJ (2014) Metal ions optical sensing by semiconductor quantum dots. Mater Chem C 2(4):595–613
33. Wang Y, Zhang C, Chen X, Yang B, Yang L, Jiang C, Zhang Z (2016) Ratiometric fluorescent paper sensor utilizing hybrid carbon dots–quantum dots for the visual determination of copper ions. Nanoscale 8(11):5977–5984
34. Ding Y, Shen SZ, Sun H, Sun K, Liu F (2014) Synthesis of l-glutathione-capped-ZnSe quantum dots for the sensitive and selective determination of copper ion in aqueous solutions. Sensors Actuators B Chem 203:35–43
35. Jiao Y, Zhou L, He H, Yin J, Gao Q, Wei J, Duan C, Peng X (2018) A novel rhodamine B-based "off-on" fluorescent sensor for selective recognition of copper (II) ions. Talanta 184:143–148
36. Wang X, Yu Z, Wang J, Shen J, Lu Y, Shen W, Lv Y, Sun X (2018) A water-soluble fluorescence "turn on" chemosensor for $Cu^{2+}$ signaling: a combined photophysical and cell imaging study. J Photochem Photobiol A 357:49–59